CHAPTER IV
RESULTS AND DISCUSSION

4.1 Plasma Treatment of PET Surface

4.1.1 Effect of Electrode Gap Distance and Plasma Treatment Time on Wettability of PET Surface

Figure 4.1 shows plasma streams occurring between the electrodes at various electrode gap distances. For the electrode gap distance of 15 mm, plasma occurred only at the edge of the electrode plates as few strong discharge streams. On the other hand, the flux of plasma increased with decreasing gap distance, and the discharge became more uniform over the entire electrode surface.

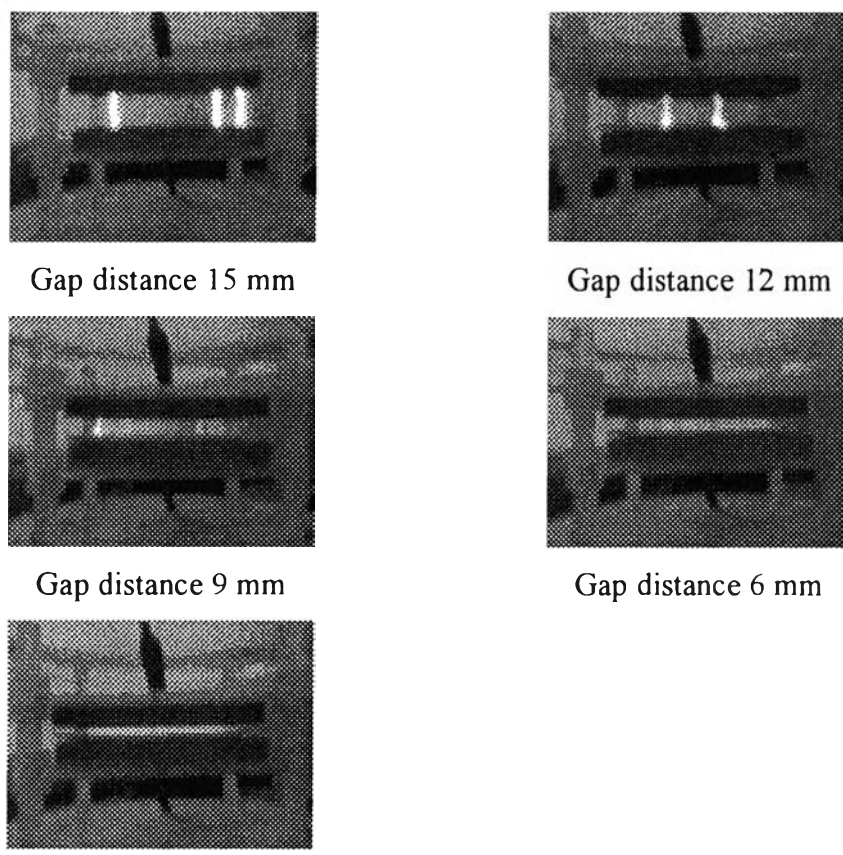

Gap distance 15 mm | Gap distance 12 mm

Gap distance 9 mm | Gap distance 6 mm

Gap distance 4 mm

Figure 4.1 Plasma generation at various electrode gap distances.

Figure 4.2 shows the effect of electrode gap distance on wettability of woven PET fabric. The time of water adsorption of the woven PET fabric decreased with decreasing electrode gap distance from 15 to 4 mm. Because the flux of plasma increased with decreasing electrode gap distance, the hydrophilicity of the woven PET fabric surface conversely increased, leading to less time required for water adsorption. However, the lowest electrode gap distance was limited at 4 mm because the woven PET fabric would directly connect to the upper and lower electrodes during being placed between the electrodes, which would cause a short circuit.

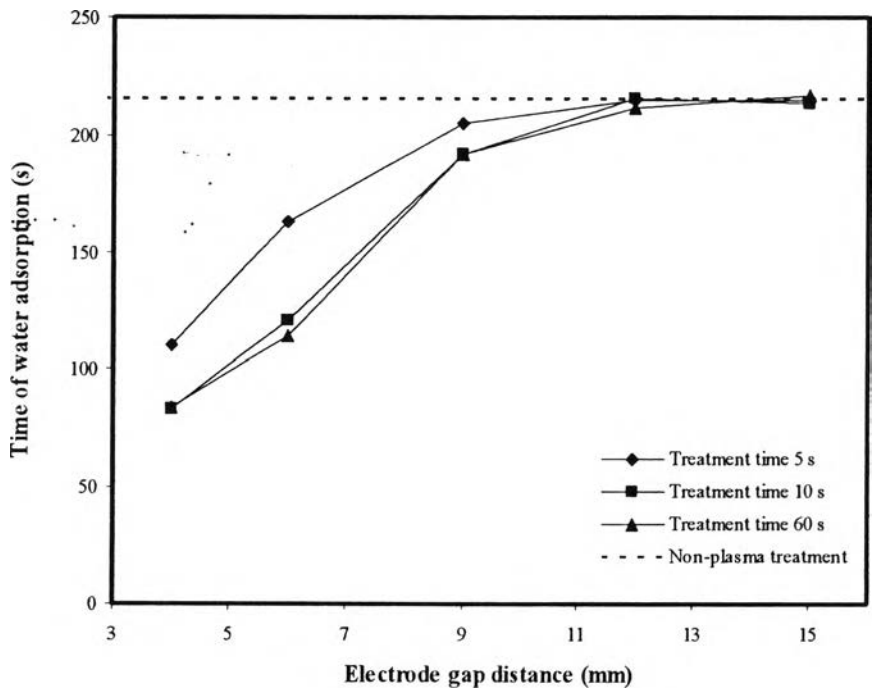

Figure 4.2 Effect of electrode gap distance on wettability of woven PET at various plasma treatment times.

The effect of treatment time on the wettability of PET surface is shown in Figure 4.3 for wickability measurement of woven PET fabric and Figure 4.4 for contact angle measurement of PET film. The time of water adsorption and contact angle of both woven PET and PET film for both measurements decreased with increasing time of plasma treatment. Increasing the treatment time of the plasma exposure resulted in a higher hydrophilic character of the woven PET fabric;

however, after a certain treatment time, a saturation level (level at which the woven PET fabric surface is completely modified) of the hydrophilicity occurred (De Geyter *et al.*, 2006). Beyond the plasma treatment of 10 s for all electrode gap distances, the time of water adsorption of the woven PET fabric became almost unchanged. Figure 4.5 shows the contact angle before and after plasma treatment for PET film. The contact angle of PET film was found to change from 79° for the as-received woven PET fabric to the lowest value of 24° after plasma treatment.

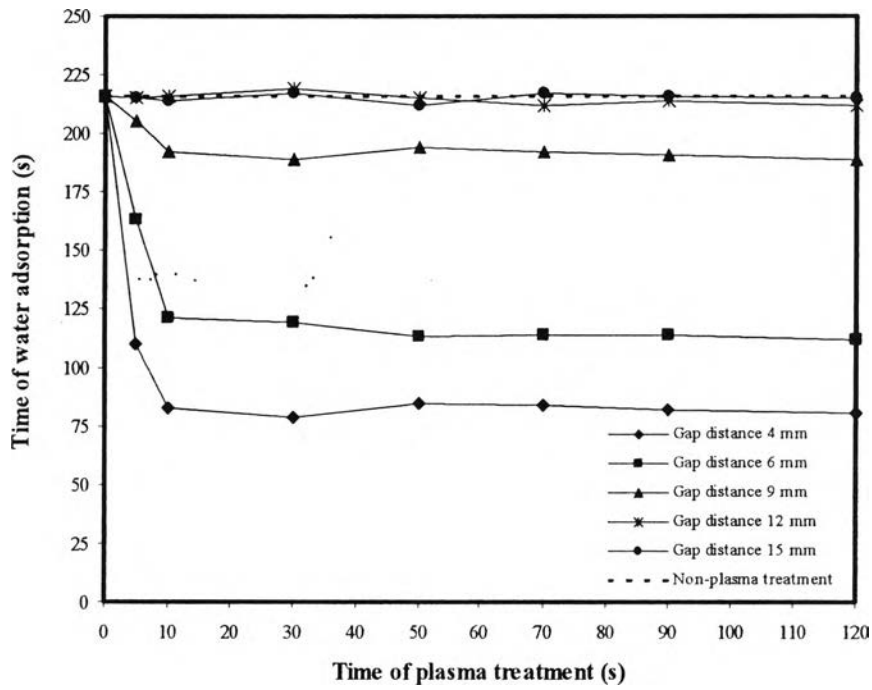

Figure 4.3 Effect of time of plasma treatment on wettability of woven PET at various electrode gap distances.

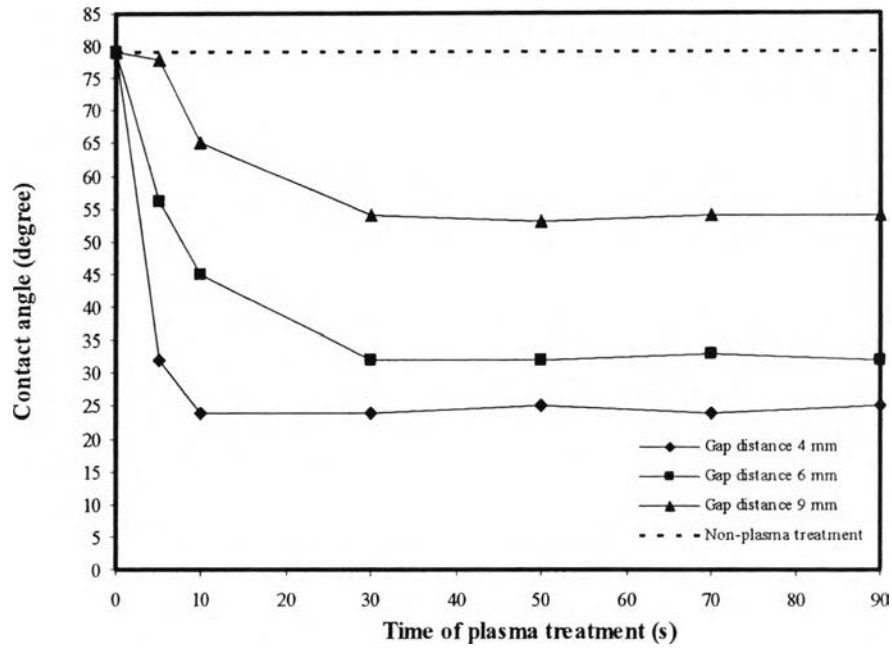

Figure 4.4 Effect of time of plasma treatment on wettability of PET film at various electrode gap distances.

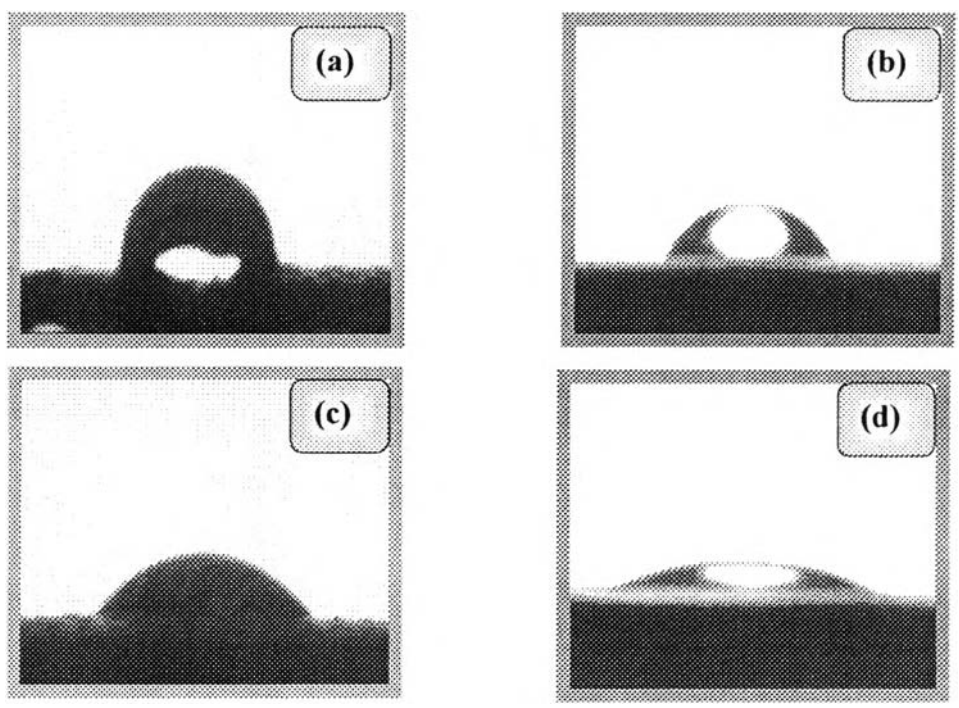

Figure 4.5 Water droplet images for contact angle measurement of (a) as-received woven PET, (b) as-received PET film (c) woven PET after plasma treatment, and (d) PET film after plasma treatment (electrode gap distance, 4 mm; treatment time, 10 s; applied voltage, 15000 V (high side); input frequency, 400 Hz).

4.1.2 Effect of Input Voltage on Wettability of PET Surface

For this part of the study, the experiments were conducted at a gap distance of 4 mm, a plasma treatment time of 10 s, a frequency of 400 Hz, and atmospheric pressure. From the experimental observation, the first point at which plasma generation occurred was 19 V, which is called the breakdown voltage. This voltage was measured at the input of the high voltage transformer.

The effect of input voltage on the wettability of woven PET fabric and contact angle of PET film is shown in Figures 4.6 and 4.7, respectively. The time of water adsorption of the woven PET fabric and contact angle measurement of PET film decreased with increasing voltage from 10 to 60 V and then remained almost unchanged. The increase in voltage results in higher electric field strength, therefore promoting higher average electron energy and electron temperature. Greater density of electrons with higher average electron energy enhances the number of inelastic collisions; therefore, it can potentially modify the surface of the woven PET fabric and PET film to be more hydrophilic. However, the time of water adsorption of woven PET fabric and contact angle measurement of PET film became almost constant when the input voltage exceeded 60 V, surface completely modified.

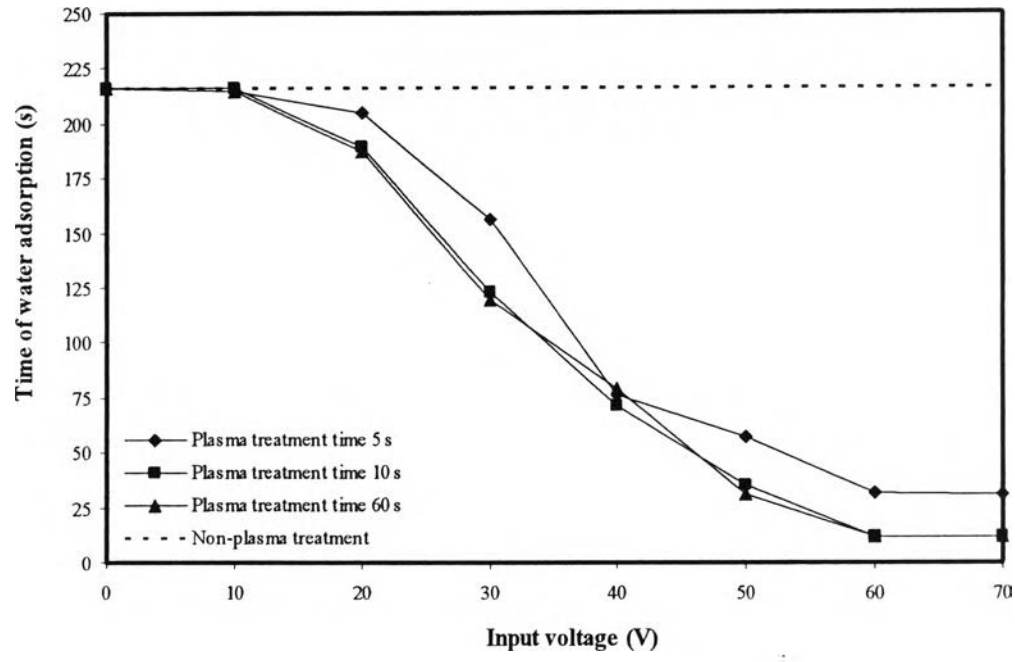

Figure 4.6 Effect of input voltage (low side) on wettability of woven PET at various plasma treatment times.

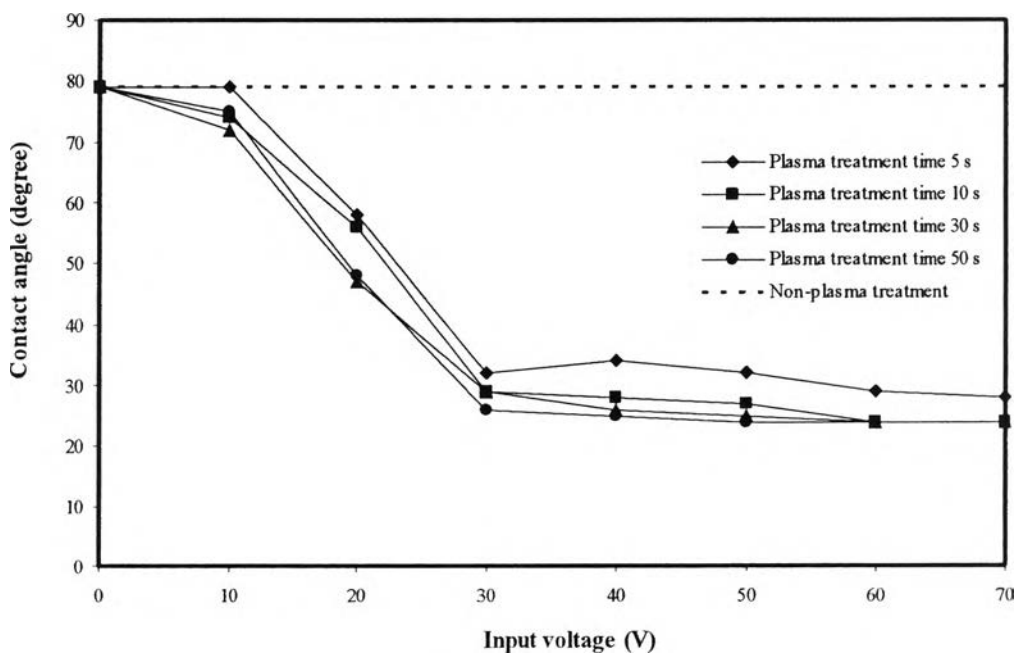

Figure 4.7 Effect of input voltage (low side) on wettability of PET film at various plasma treatment times.

From XPS characterization, a DBD discharge under air atmospheric can generate a wide range of active species, including atomic oxygen, ozone, nitrogen oxides, neutral and meta-stable molecules, radicals, and ultraviolet radiation. An air plasma increases the surface energy of polymers and textiles by introducing oxygen-containing polar groups onto the polymer surface. Atomic oxygen is believed to be the main reactive species responsible for this oxygen inclusion (Kogelschatz, 2003). Atomic oxygen is formed because of the dissociation of O_2 molecules by electron impact. However, excitation and dissociation of nitrogen molecules also lead to a number of additional reaction paths that can produce additional atomic oxygen (Fang *et al.*, 2001). To investigate what functional groups were formed by plasma treatment, the surface characteristic of the untreated and plasma-treated samples was examined by XPS.

Figure 4.8 shows the C1s spectra of woven PET fabric surface before and after plasma treatment. The C1s spectra of the woven PET were deconvoluted into 4 components: one at 285.0 eV due to the C–C and C–H groups, one at 286.7 eV due to the CH_2–O– group, one at 289.0 eV due to the O–C=O group, and one at 283.3 eV, which could not be attributed to any specific chemical group. However, it is also possible that the component at 283.3 eV was the result of the broadening of the C1s peak caused by the strong charging of the polyester during the XPS measurements.

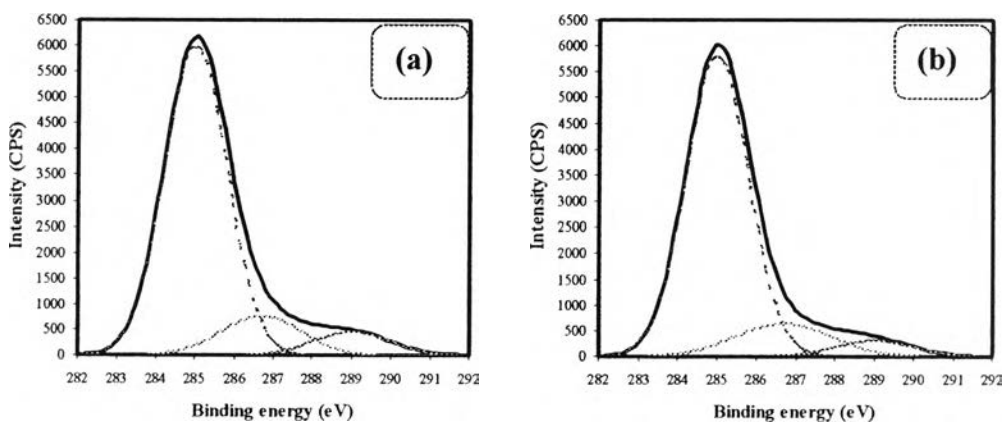

Figure 4.8 Deconvoluted C1s XPS spectra of woven PET (a) before plasma treatment and (b) after plasma treatment (electrode gap distance, 4 mm; treatment time, 10 s; input voltage, 60 V (low side); input frequency, 400 Hz)

Figure 4.8(a) shows the functional group distribution of the as-received woven PET fabric as a function of energy density. The as-received woven PET fabric contained 9.81% C–O group, 2.96% O–C=O group, and 76.72% C–C and C–H groups. The phenyl group on the woven PET fabric surfaces is not presented in Figure 4.8(a). The concentration of the oxidized carbon components (C–O and O–C=O) increased with increasing energy density after plasma treatment at atmospheric pressure until a saturation level was reached (De Geyter *et al.*, 2006).

Figure 4.8(b) also shows that after plasma treatment at atmospheric pressure, the concentration of the C–O and O–C=O groups increased to 12.42 and 8.21%, respectively, while the concentration of the C–C and C–H groups decreased to approximately 68.21%. This means that the air plasma mainly attacks the C–C and C–H groups rather than the ester groups in the polymer chains to form more O–C=O and C–O groups. The introduction of these polar O–C=O and C–O groups is responsible for the higher hydrophilicity of the woven PET fabric after plasma treatment.

It is shown that an increasing power resulted in a higher hydrophilic character. This was not only caused by the presence of more active species at higher power, but also by the behavior of the barrier discharge itself. At higher discharge power, more microdischarges are present, and the distance between individual microdischarges decreases, which also results in a better plasma treatment (De Geyter *et al.*, 2006).

4.1.3 Effect of Frequency on Wettability of PET Surface

For this part of the study, the experiments were conducted at a gap distance of 4 mm, a plasma treatment time of 10 s, and atmospheric pressure, whereas voltage and frequency were varied. The effect of applied frequency on the wettability of the woven PET fabric is shown in Figure 4.9. At 60 V, it was experimentally observed that the initial point of frequency for plasma generation was 60 Hz, and the maximum point was 350 Hz. Beyond this maximum value of frequency, the flux of plasma decreased with increasing frequency. The last point of frequency where plasma still existed was 650 Hz. The effect of frequency on plasma generation at various voltages is shown in Table 4.1.

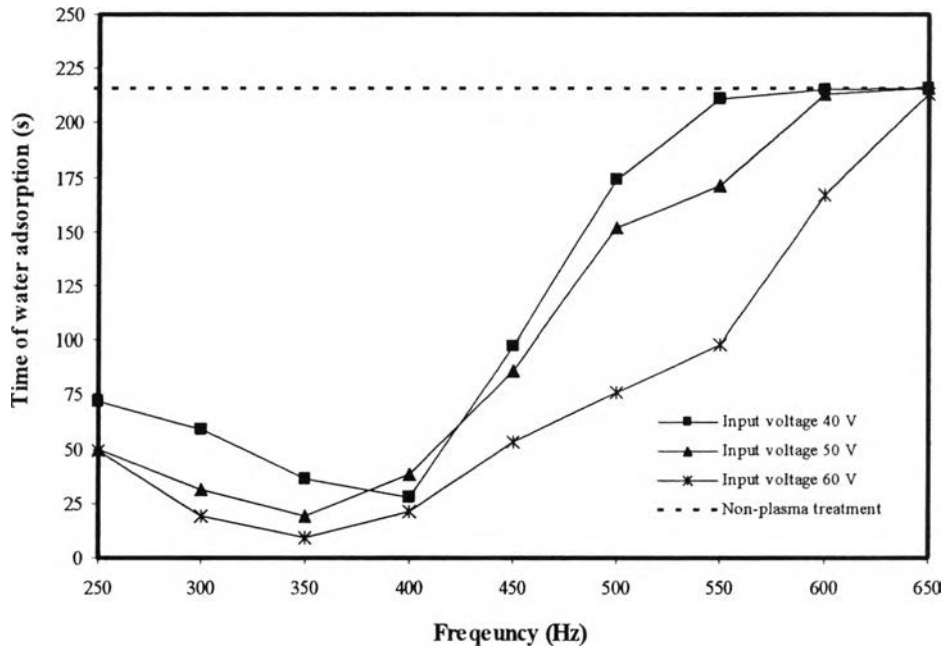

Figure 4.9 Effect of frequency on wettability of woven PET at various input voltages.

Table 4.1 Effect of frequency on plasma generation at various voltages

Input voltage (V)	Initial frequency value to generate plasma (Hz)	Frequency value to generate maximum plasma (Hz)	Final frequency value to generate plasma (Hz)
30	290	415	540
40	110	400	550
50	70	365	570
60	60	350	650

The explanation is that a higher frequency results in lower current, which corresponds to the reduction of the number of electrons generated (Morinaga and Suzuki, 1961 and 1962), as confirmed by less hydrophilicity due to higher time required for water adsorption, shown in Figure 4.9. Consequently, the opportunity of collision between electrons and O_2 molecules decreased, and therefore the wettability of woven PET fabric decreased as well.

4.1.4 Effect of Plasma Treatment on Physical Properties of Woven PET

Figure 4.10 shows SEM images of woven PET surface with (a) Non-plasma treatment (b) After plasma treatment: electrode gap distance, 4 mm; treatment time, 10 s; applied voltage, 60 V (low side); input frequency, 400 Hz. It showed that plasma did not destroy surface of woven PET fabric.

During the tensile test the distance between two clamps was kept 200 mm and the crosshead displacement was set 10 mm/min. The results of the tensile strength test are summarized in Table 4.2. Each datum in Table 4.2 is the mean of 5 measurements. It is seen in the table that the tensile strength of woven PET fabric after plasma treatment slightly changes when compares with as-received woven PET fabric. It is clearly that plasma did not much change physical property of woven PET.

Table 4.2 Tensile strength of as-received woven PET and woven PET after plasma treatment

Materials	Breaking strength (N)	Elongation at break (%)
As-received woven PET	44.8	41.2
Woven PET after plasma treatment	43.8	37.7

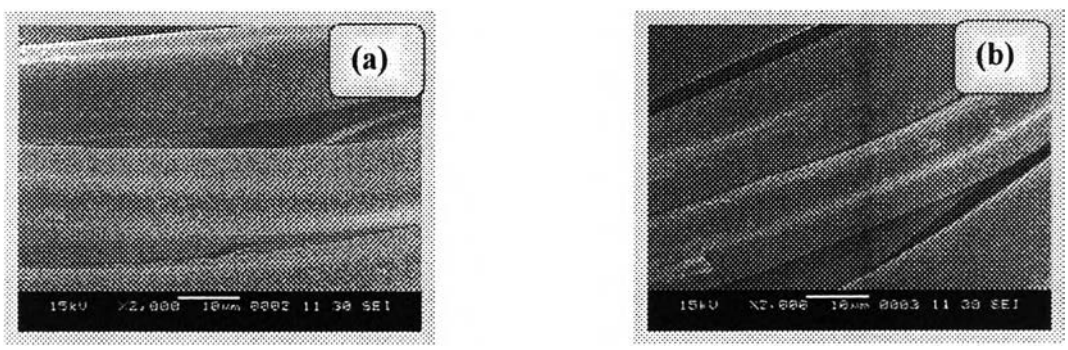

Figure 4.10 SEM images of woven PET surface with (a) Non-plasma treatment (b) After plasma treatment: electrode gap distance, 4 mm; treatment time, 10 s; applied voltage, 60 V (low side); input frequency, 400 Hz.

4.1.5 Effect of Type of Gas Feed on Wettability of PET Surface

In this section, the experiments were conducted at a gap distance of 4 mm, a plasma treatment time of 10 s, a frequency of 345 Hz, and atmospheric pressure, whereas voltage and type of gas feed were varied. The effects of type of gas feed, including air, O_2, N_2, and Ar, on the wettability of woven PET fabric and contact angle of PET film are shown in Figures 4.11 and 4.12, respectively. The time of water adsorption of woven PET fabric decreased with increasing voltage in the range of 10 to 50 V and then remained almost unchanged. All types of gas feed caused the increase in hydrophilicity of the woven PET fabric surface in the order of air $\approx O_2 >$ Ar $> N_2$. On the other hand, the contact angle of PET film decreased with increasing voltage in the range of 10 to 60 V and then remained almost unchanged. The type of gas feed caused the increase in hydrophilicity of the PET film in the order of air $\approx O_2 \approx$ Ar $> N_2$.

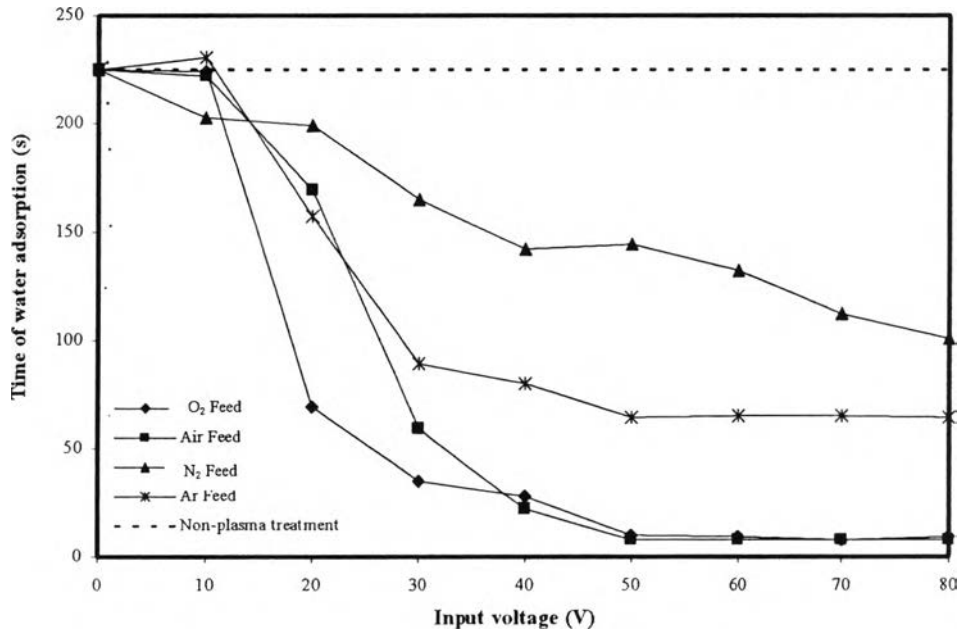

Figure 4.11 Effect of type of gas feed on wettability of woven PET at various input voltages.

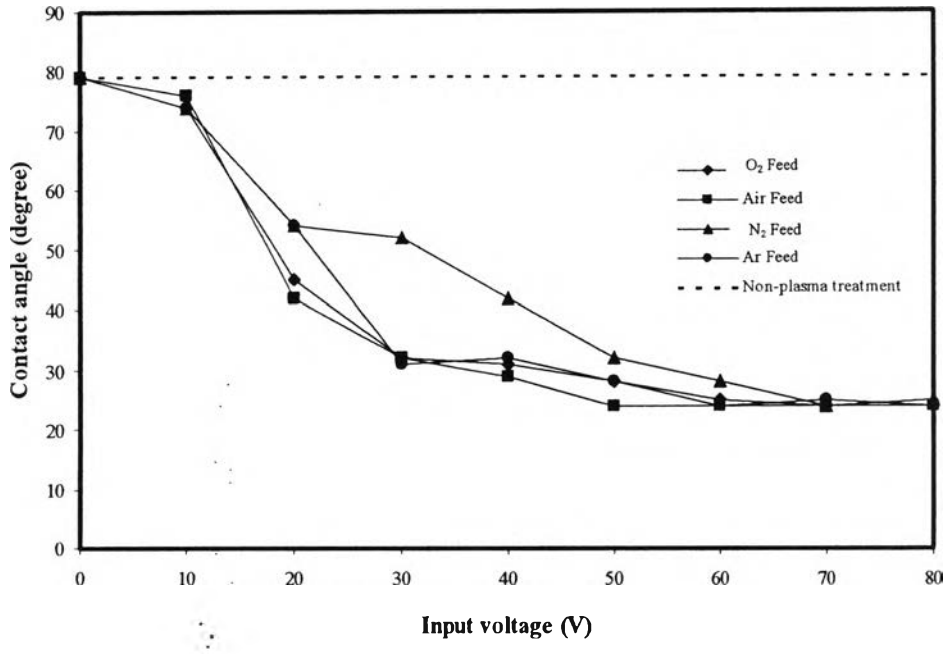

Figure 4.12 Effect of type of gas feed on wettability of PET film at various input voltages.

To determine the chemical nature of the surface structure, the infrared spectroscopy with adaptation for the rough surfaces was used. The as-received woven PET fabric and woven PET after plasma treatment under various gases were submitted to FTIR analysis. The FTIR spectra of PET film and woven PET fabric are shown in Figures 4.13 and 4.14, respectively. The results show that the most changes between the as-received woven PET fabric and woven PET fabric after plasma treatment under various gases are in the wavenumber range of 400–4000 cm^{-1}. It is also evident that the peak intensity at 732 cm^{-1}, which is attributed to aromatic C–H bond, increased after plasma treatment, especially under air-plasma treatment, but the peak intensity between 2900-2980 cm^{-1}, which is attributed to aliphatic C–H bond, slightly decreased. In addition, the wavenumbers of 1142 and 1730 cm^{-1} can be attributed to C–O and C=O, respectively. After air-plasma treatment, there is a substantial increase in peak intensity at 1260 cm^{-1}, which can be attributed to the O–C=O. Since an oxygen plasma increases the surface energy of polymers and textiles by introducing oxygen-containing polar groups onto the polymer surface, atomic

oxygen is believed to be the main reactive species responsible for this oxygen inclusion (De Geyter *et al.*, 2006). However, when increasing to high voltage in the case of pure O_2, oxygen molecules become fragmented into many active species; and the active species of oxygen may recombine to oxygen molecule due to its high density. This may reduce the total available active species in the case of pure oxygen. On the other hand, air can generate more active species than oxygen because when increasing voltage, both nitrogen and oxygen molecules also become fragmented into many active species. Although nitrogen dose not play a significant role in changing the functional groups of woven PET fabric surface, but nitrogen is still an active gas. Active species of nitrogen can possibly collide with oxygen molecule to easily generate more active species. When increasing active species of oxygen, more new functional groups on polymer surface could be obtained, resulting in higher hydrophilicity of woven PET fabric surface.

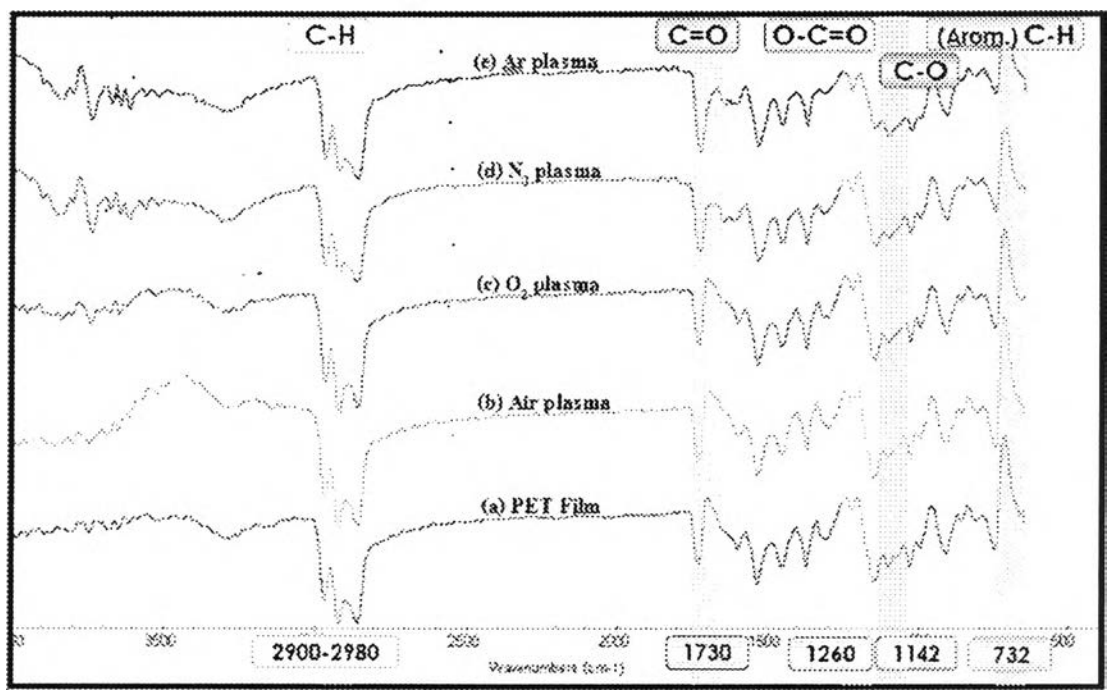

Figure 4.13 FT-IR spectra of PET film at atmospheric pressure with (a) non-plasma treatment, (b) air-plasma treatment, (c) O_2-plasma treatment, (d) Ar-plasma treatment, and (e) N_2-plasma treatment.

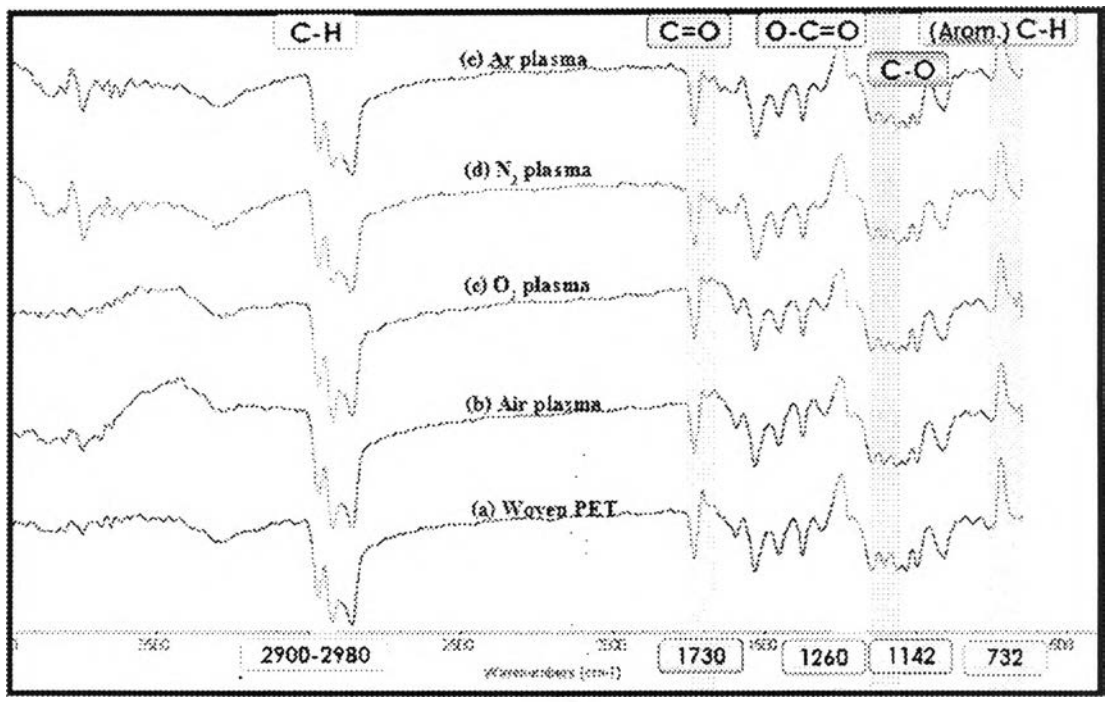

Figure 4.14 FT-IR spectra of woven PET at atmospheric pressure with (a) non-plasma treatment, (b) air-plasma treatment, (c) O_2-plasma treatment, (d) Ar-plasma treatment, and (e) N_2-plasma treatment.

4.1.6 Effect of Type of Gas Feed under Vacuum on Wettability of PET Surface

The experiments under vacuum were operated after evacuating air from the chamber until the pressure reached 0.04 bar. After that, gas was fed into the chamber until the pressure reached 0.15 bar. For this experimental section, experiments were conducted at a gap distance of 4 mm, a plasma treatment time of 10 s, a frequency of 345 Hz, whereas voltage and type of gas feed were varied. The effects of type of gas feed, including air, O_2, N_2, and Ar, on the wettability of woven PET fabric and contact angle of PET film are shown in Figures 4.15 and 4.16, respectively. The time of water adsorption of the woven PET fabric decreased with increasing voltage from 10 to 40 V and then remained almost unchanged. The type of gas feed caused the increase in hydrophilicity of the woven PET fabric surface in the order of air $\approx O_2 > Ar > N_2$. On the other hand, the contact angle of PET film decreased with increasing voltage in the range of 10 to 30 V and then remained almost unchanged. However, the type of gas feed did not cause the significant in

hydrophilicity of the PET film. In the case of oxygen, time of water adsorption remained almost unchanged when increasing input voltage more than 40 V. For this situation, in which air was evacuated, the number of gas molecules inside the chamber was therefore lower than those at atmospheric pressure. So, plasma occurred much easier because the resistance between the electrodes was decreased. This result is similar to the work of Borcia *et al.* (2004), which reported that a polyester film treated in air using a DBD at atmospheric pressure resulted in a relative variation of the oxygen content of 31.7%. This means that working with a DBD at medium pressure seems to be more efficient in increasing oxygen content than working at atmospheric pressure. The increase in oxygen content suggests that new oxygen-containing polar groups are formed on the woven PET surface. The relative oxygen content on the surface will not further increase after a certain treatment time, resulting in a saturation state of the wettability (De Geyter *et al.*, 2006). This means that at saturation, a limiting level of oxidation of the sample surface was reached.

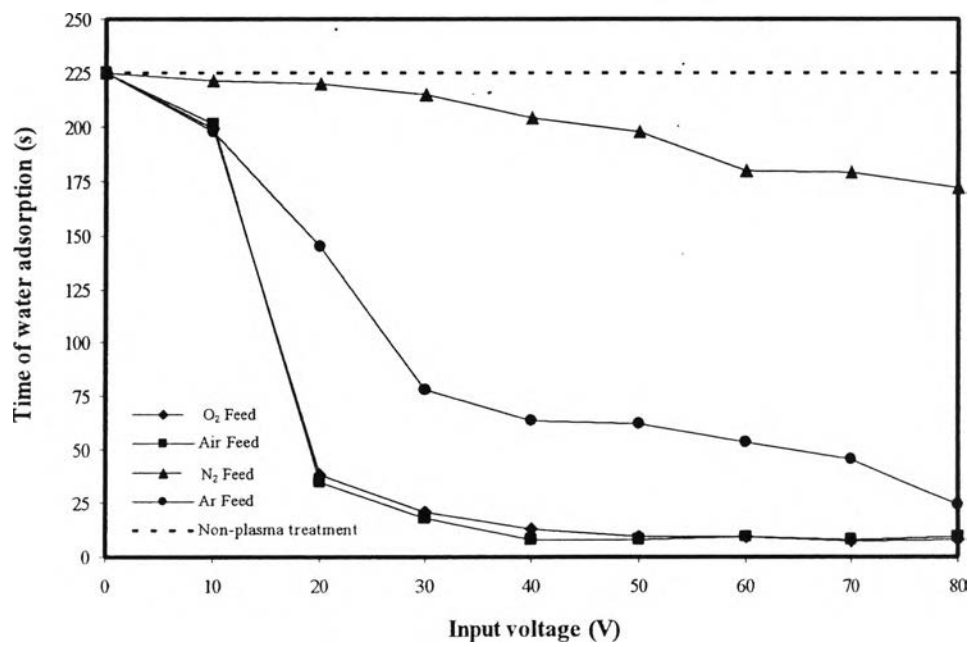

Figure 4.15 Effect of type of gas feed under pressure of 0.15 bar on the wettability of woven PET fabric at various input voltages.

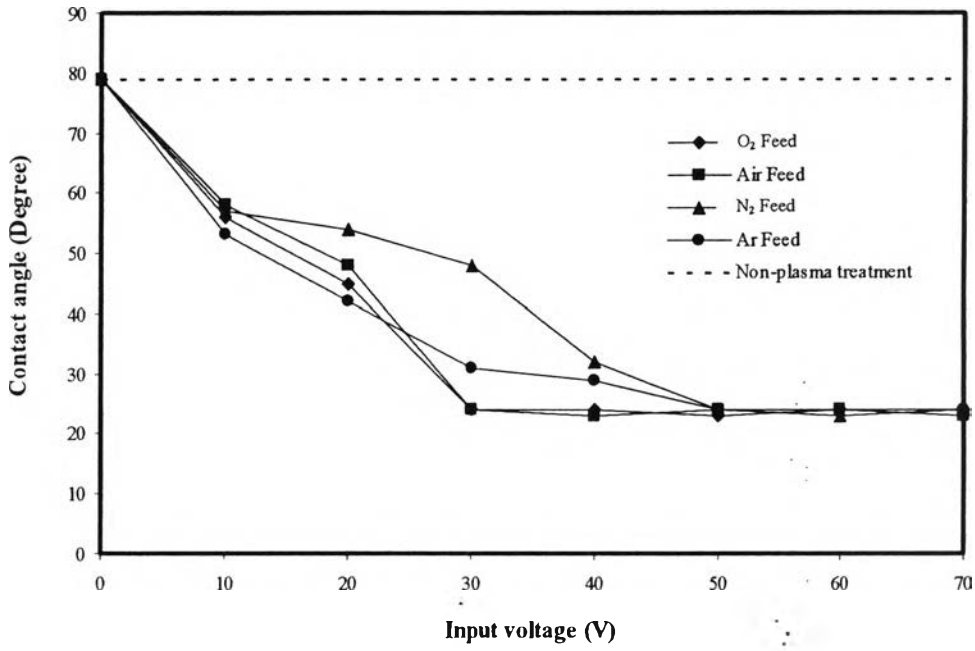

Figure 4.16 Effect of type of gas feed under pressure of 0.15 bar on the wettability of PET film at various input voltages.

The FTIR spectra of PET film and woven PET fabric are shown in Figures 4.17 and 4.18, respectively. The results show that the most changes between the as-received woven PET and woven PET after plasma treatment in various gases are in the wavenumber range of 400–4000 cm^{-1}. It is also evident that the peak intensity at 732 cm^{-1}, which corresponds to aromatic C–H bond, increased after plasma treatment, especially under air-plasma treatment, whereas the peak intensity between 2900-2980 cm^{-1}, which is due to aliphatic C–H bond, slightly decreased. In addition, the wavenumbers of 1142 and 1730 cm^{-1} can be attributed to C–O and C=O, respectively, as above mentioned. After air plasma treatment, there is a substantial increase in peak intensity at 1260 cm^{-1}, which corresponds to the O–C=O bond.

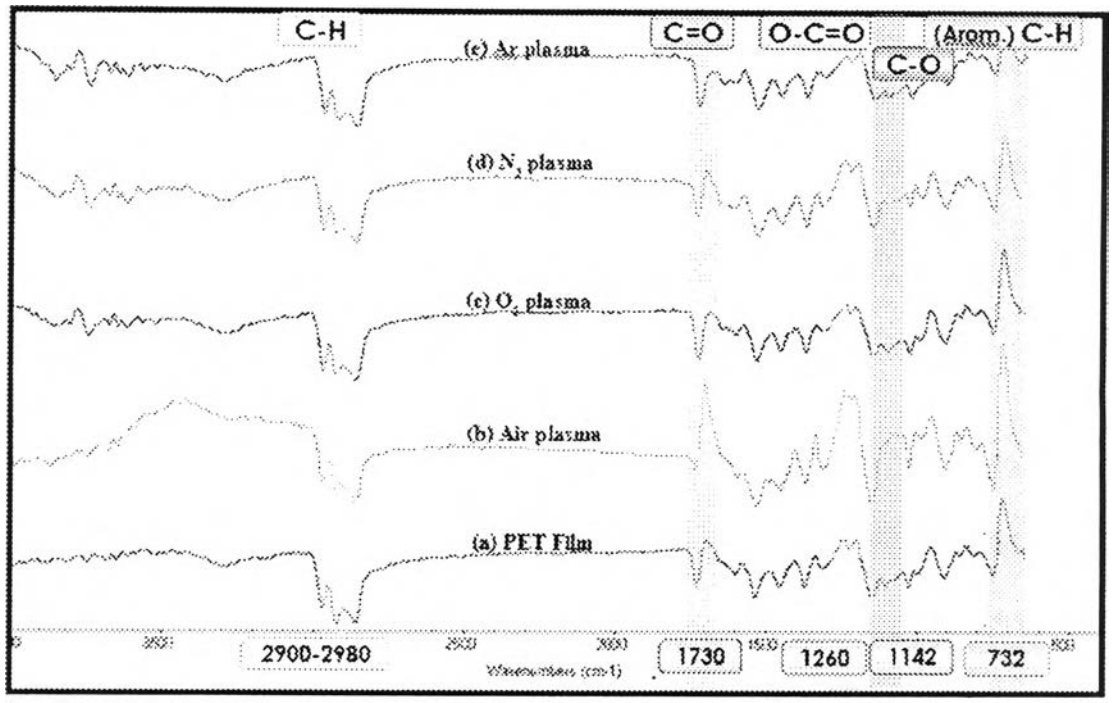

Figure 4.17 FT-IR spectra of PET film under pressure of 0.15 bar with (a) non-plasma treatment, (b) air-plasma treatment, (c) O_2-plasma treatment, (d) Ar-plasma treatment, and (e) N_2-plasma treatment.

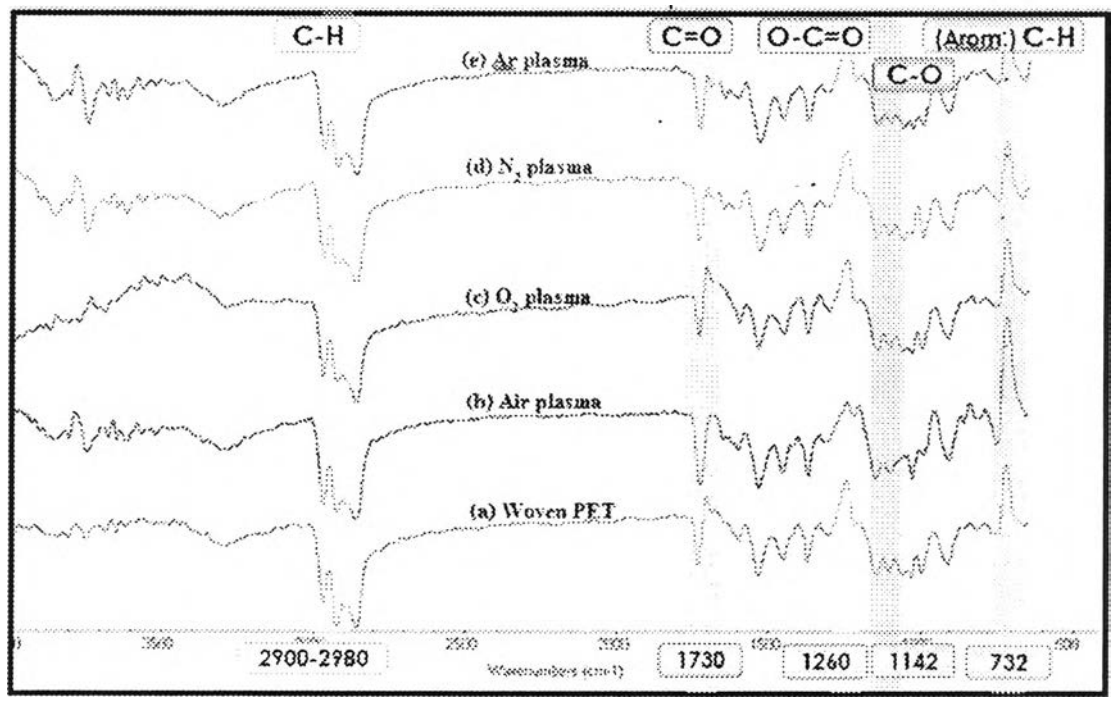

Figure 4.18 FT-IR spectra of woven PET under pressure of 0.15 bar with (a) non-plasma treatment, (b) air-plasma treatment, (c) O_2-plasma treatment, (d) Ar-plasma treatment, and (e) N_2-plasma treatment.

De Geyter *et al.* (2007) also studied the PET surface modification by using DBD plasma technique. They found that plasma treatment at medium pressure led to a faster decrease in the C–C and C–H bonds and a faster increase in the oxidized carbon bonds than at atmospheric pressure. However, at higher energy densities, the evolution of the functional groups on the PET surface is quite similar for both pressure conditions. At low energy densities, a medium pressure plasma treatment is more energy-efficient in incorporating oxygen on the surface than an atmospheric pressure plasma treatment. This effect could be explained by the larger diameter of the micro-discharges and the lower quenching rate of atomic oxygen at medium pressure. The results also show that at energy densities higher than ±200 mJ/cm^2, no significant difference can be observed between medium and atmospheric pressure plasma treatments. AFM images of the medium and atmospheric pressure plasma-treated PET films showed that the water contact angle of the films can decrease to a minimum without causing significant physical degradation of the surface.

4.2 Silver Deposition on Plasma-Treated PET Surface and Antimicrobial Activity Test

4.2.1 Effect of Number of Washing Cycle on Amount of Deposited Silver

Figure 4.19 shows the relation between the number of washing cycle and amount of deposited Ag characterized by atomic absorption spectroscopy. In case of coating with 3 M $AgNO_3$ solution, the result shows that the amount of silver deposited on woven PET slightly decreased with increasing the number of washing cycle. After washing woven PET for three times, amount of silver on woven PET fabric was constant. On the other hand, in case of coating with 0.05 and 1 M $AgNO_3$ solutions, the amount of silver deposited on woven PET fabric slightly decreased with increasing number of washing cycle, but amount of silver on woven PET fabric was also constant after washing woven PET fabric for three times.

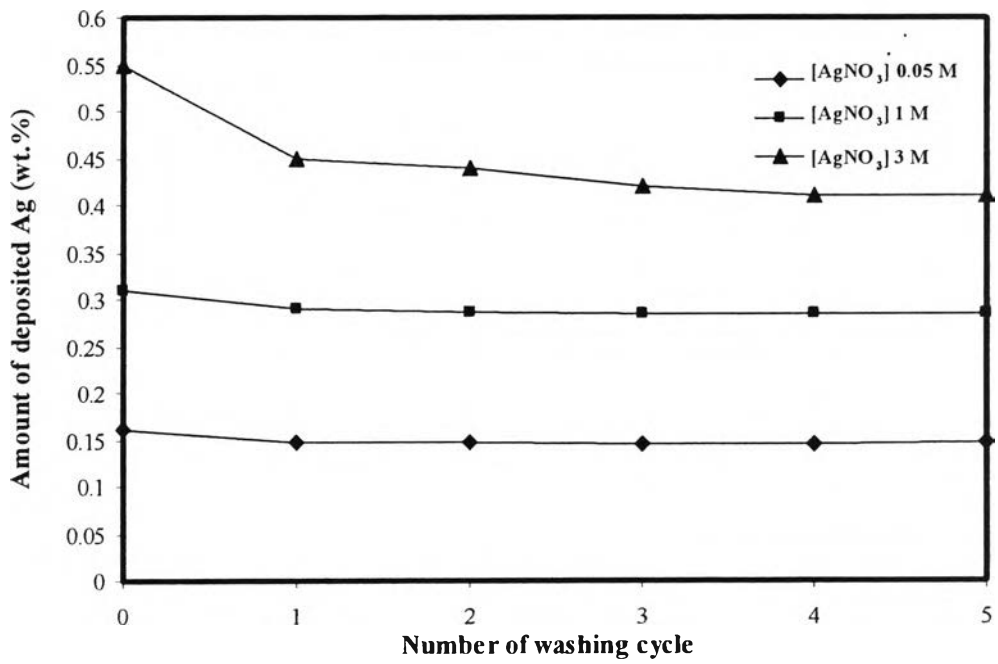

Figure 4.19 Effect of number of washing cycle on amount of silver deposited on woven PET at various $AgNO_3$ concentrations.

4.2.2 Saturated Amount of Silver Deposited on Woven PET Fabric

Characterization results from atomic absorption spectroscopy were used to find saturated amount of silver on woven PET fabric. Figure 4.20 shows the relation between the amount of silver deposited on woven PET fabric and $AgNO_3$ concentration used for Ag deposition. The results show that the amount of silver deposited on woven PET fabric increased with increasing concentration of $AgNO_3$ from 0.01 to 3 M and then remained almost unchanged. Therefore, the saturated amount of silver deposited on woven PET was 0.41 wt.%.

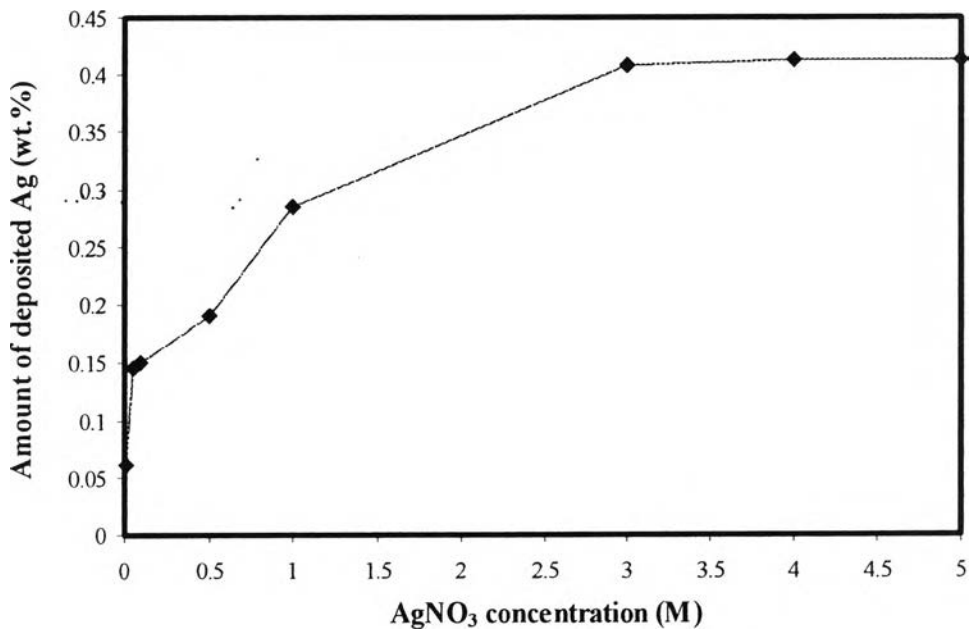

Figure 4.20 Effect of $AgNO_3$ concentration on amount of silver deposited on woven PET.

4.2.3 Effect of $AgNO_3$ Concentration on Size of Silver Deposited on Woven PET

Figure 4.21 shows the UV-visible spectra of woven PET surface coated with Ag nanoparticles by using various concentrations of silver nitrate. At the $AgNO_3$ concentration of 0.05 M, a symmetrical absorption band is located at 420 nm, which is the typical absorption band of metallic silver nanoparticles due to the surface plasmon resonance (SPR) (Kim *et al.*, 2004). This implies that the small silver nanoparticles with the narrow size distribution were formed. The absorption band slightly broadened with increasing concentration of $AgNO_3$. The absorption band became much broadened at the $AgNO_3$ concentration of 1 M. The broadening of absorption band is possible to show an increase in the particle size and size distribution (Sconichsen *et al.*, 2002). This suggests that the larger silver nanoparticles with the wider size distribution were probably formed when the concentration of $AgNO_3$ was increased, resulting from the silver ion aggregation. In order to obtain the particle size of deposited silver, SEM analysis was also performed. Figure 4.22(a) and (b) show morphology of as-received PET film and silver-coated plasma-treated PET film, respectively. The size dispersion of silver on PET film is in the range of 40 – 120 nm.

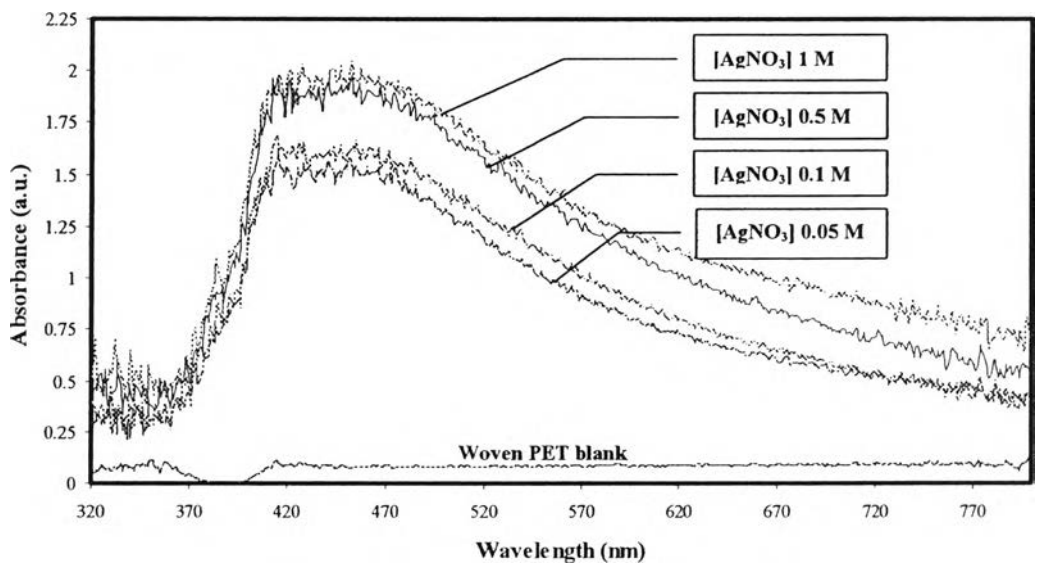

Figure 4.21 UV-visible spectra of woven PET coated with various $AgNO_3$ concentrations.

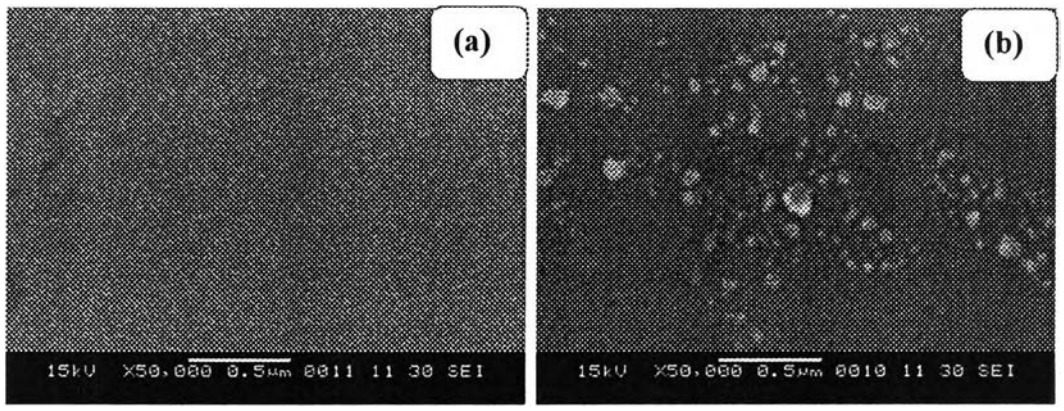

Figure 4.22 SEM images of PET film (a) without Ag coating and (b) with Ag coating at $AgNO_3$ concentration of 0.05 M.

The silver-coated plasma-treated woven PET was also characterized by XPS technique. Figure 4.23(a) shows the C1*s* core level spectra resolved into three individual component peaks: first peak at 285.0 eV, which can be attributed to the carbon in C–C or C–H groups; second peak at 286.7 eV, corresponding to CH_2–O; and third peak at 289.0 eV, due to O–C=O (De Geyter *et al.*, 2006). Figure 4.23(b) shows the O1*s* spectra resolved into three individual component peaks: first peak at 531.5 eV, attributed to the presence of metal–O formed during the oxidation treatment process; second peak at 532.51eV, attributed to the presence of C–OH or COOH groups; and third peak at 534.5eV, attributed to oxygen in the metal–OH (Park *et al.*, 2007). And, Figure 4.23(c) shows the high-resolution Ag3*d*5/2 spectra resolved into two individual component peaks: first peak at 367.95 eV, corresponding to deposition of silver as Ag_2O (Weaver and Hoflund, 1994); and second peak at 368.85 eV, due to the presence of isolated zero-valence silver atoms deposited on the PET surface (Biniak *et al.*, 1999).

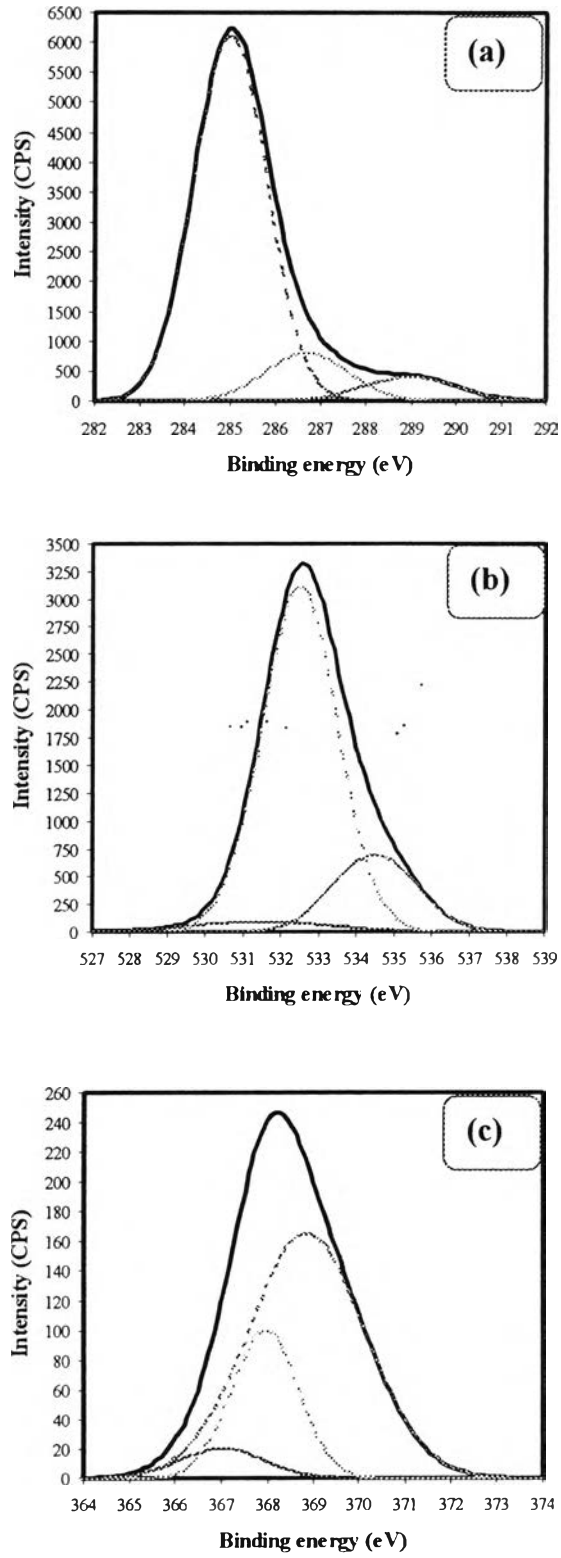

Figure 4.23 Deconvoluted XPS spectra of woven PET with air-plasma treatment (a) C1s, (b) O1s, and (c) Ag 3d5/2 of woven PET coated with Ag using [$AgNO_3$] of 0.05 M.

4.2.4 Effect of $AgNO_3$ Concentration and $NaBH_4$ Treatment on Clear Zone Distance

For this experimental section, experiments were conducted at a gap distance of 4 mm, a plasma treatment time of 10 s, a input voltage of 50 V (low side), a frequency of 345 Hz, a pressure 0.15 bar, air feed, whereas $AgNO_3$ concentration was varied to find the condition that exhibited a clear zone (antimicrobial testing).

The plasma-treated woven PET fabric was comparatively coated with silver by two methods. For the first method, the woven PET fabric was submerged into $AgNO_3$ aqueous solution and subsequently dipped into $NaBH_4$ aqueous solution. For the second one, the woven PET was only submerged into $AgNO_3$ aqueous solution without $NaBH_4$ treatment.

The effect of $AgNO_3$ concentration on the antimicrobial activity of woven PET fabric coated with silver by the two aforementioned methods is shown in Figure 4.24. The antimicrobial activity of woven PET fabric (clear zone range) increased with increasing $AgNO_3$ concentration in the studied range of 0.01 to 1 M. In the case where the woven PET fabric was submerged into both $AgNO_3$ and $NaBH_4$ solutions, there was no clear zone observed for all $AgNO_3$ concentrations. From the AAS results, the amount of silver on woven PET fabric, which was submerged into both 0.05 M $AgNO_3$ solution and 0.1 M $NaBH_4$ solution, was only 0.032 wt.%. On the other hand, amount of silver on woven PET fabric, which was only submerged into 0.05 M $AgNO_3$ solution, was 0.146 wt.%. The results showed that silver deposited on woven PET surface was leached from PET surface by being dissolved in the $NaBH_4$ solution. Therefore, it causes a significant decrease in antimicrobial performance of woven PET fabric.

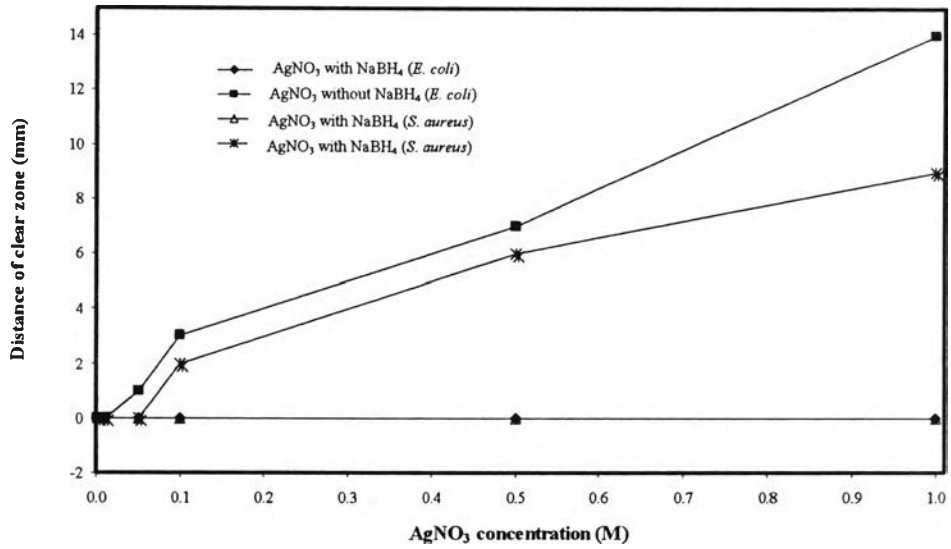

Figure 4.24 Effect of $AgNO_3$ concentration without and with treatment by 0.1 M $NaBH_4$ on clear zone distance.

4.2.5 Antimicrobial Activity Testing

4.2.5.1 The Disk Diffusion Method

The antibacterial activity of silver-coated plasma-treated woven PET fabric for *E. coli* and *S. aureus* was measured by the disk diffusion method. It was found that woven PET with deposited Ag nanoparticles exhibited an inhibition zone. Figure 4.25 shows that woven PET fabric, which was only submerged into $AgNO_3$ solution, exhibited a clear zone at the $AgNO_3$ concentration of 0.01 M in the case of *E. coli* and 0.05 M in the case of *S. aureus*. Antibacterial efficiency against *S. aureus* was lower than that against *E. coli*, probably because of the difference in cell wall characteristic between gram-positive and gram-negative bacteria.

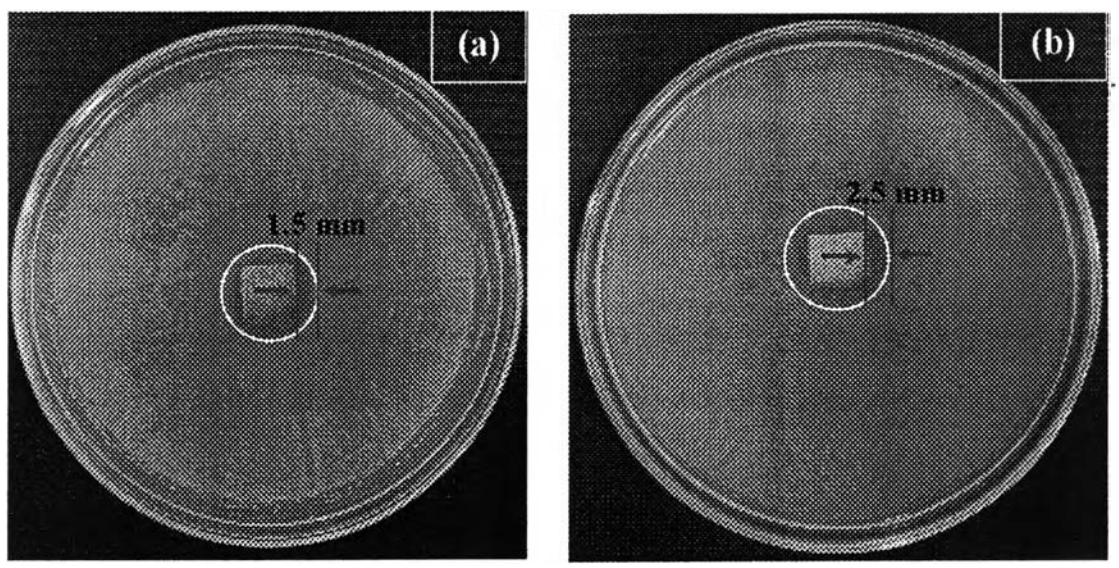

Figure 4.25 The antibacterial activity of plasma-treated woven PET against (a) *E. coli* (woven PET coated with Ag using [$AgNO_3$] of 0.01 M) and (b) *S. aureus* (woven PET coated with Ag using [$AgNO_3$] of 0.05 M)

4.2.5.2 The Colony Forming Count Method

The silver-coated plasma-treated woven PET was also tested for antimicrobial activity against *E. coli* and *S. aureus* by using the colony forming count method. No bacterial growth was observed from the sterility control. The viable counts recovered from the silver-coated plasma-treated woven PET fabric before and after incubation are shown in Table 4.3. After 48 h of incubation, there was a 99.99 % reduction in viable *E. coli* and *S. aureus* on the silver-coated plasma-treated woven PET. For as-received woven PET fabric, there was no reduction in viable counts; on the contrary, there were 13.16 and 15.12 % increases in the viable cell counts of *E. coli* and *S. aureus*, respectively.

Table 4.3 Colony forming unit counts (cfu/mL) at 0-h and 24-h contact time intervals with silver coating after plasma treatment of woven PET against *E. coli* and *S. aureus*

Contact time	*E. coli*			*S. aureus*		
	Ag coated-woven PET	Woven PET	Blank	Ag coated-woven PET	Woven PET	Blank
0 h	3.8×10^{7}	3.8×10^{7}	3.8×10^{7}	3.44×10^{7}	3.44×10^{7}	3.44×10^{7}
24 h	1.12×10^{3}	4.3×10^{7}	5.6×10^{7}	6.4×10^{2}	3.96×10^{7}	5.18×10^{7}
% of reduction / increase	99.99% reduction	13.16% increase	47.37% increase	99.99% reduction	15.12% increase	50.58% increase